Neurochemistry International 80 (2015) 110–119

Contents lists available at ScienceDirect

Neurochemistry International

journal homepage: www.elsevier.com/locate/nci

Di-*O*-demethylcurcumin protects SK-N-SH cells against mitochondrial and endoplasmic reticulum-mediated apoptotic cell death induced by $A\beta_{25-35}$

Decha Pinkaew [a], Chatchawan Changtam [b], Chainarong Tocharus [c], Sarinthorn Thummayot [c], Apichart Suksamrarn [d], Jiraporn Tocharus [a,*]

[a] Department of Physiology, Faculty of Medicine, Chiang Mai University, Chiang Mai 50200, Thailand
[b] Division of Physical Science, Faculty of Science and Technology, Huachiew Chalermprakiet University, Samutprakarn 10540, Thailand
[c] Department of Anatomy, Faculty of Medicine, Chiang Mai University, Chiang Mai 50200, Thailand
[d] Department of Chemistry and Center of Excellence for Innovation in Chemistry, Faculty of Science, Ramkhamhaeng University, Bangkok 10240, Thailand

ARTICLE INFO

Article history:
Received 2 July 2014
Received in revised form 20 October 2014
Accepted 21 October 2014
Available online 24 October 2014

Keywords:
Alzheimer's disease
Amyloid beta
Apoptosis
Di-*O*-demethylcurcumin
Endoplasmic reticulum stress
Mitochondrial death pathway

ABSTRACT

Alzheimer's disease (AD) is a neurodegenerative and progressive disorder. The hallmark of pathological AD is amyloid plaque which is the accumulation of amyloid β (Aβ) in extracellular neuronal cells and neurofibrillary tangles (NFT) in neuronal cells, which lead to neurotoxicity via reactive oxygen species (ROS) generation related apoptosis. Loss of synapses and synaptic damage are the best correlates of cognitive decline in AD. Neuronal cell death is the main cause of brain dysfunction and cognitive impairment. Aβ activates neuronal death via endoplasmic reticulum (ER) stress and mitochondria apoptosis pathway. This study investigated the underlying mechanisms and effects of di-*O*-demethylcurcumin in preventing Aβ-induced apoptosis. Pretreatment with di-*O*-demethylcurcumin for 2 h, which was followed by $A\beta_{25-35}$ (10 μM) in human neuroblastoma SK-N-SH cells improved cell viability by using MTS assay and decreased neuronal cell apoptosis. Pretreatment with di-*O*-demethylcurcumin attenuated the number of nuclear condensations and number of apoptotic cells in $A\beta_{25-35}$-induced group in a concentration-dependent manner by using transmission electron microscope (TEM) and flow cytometry, respectively. Di-*O*-demethylcurcumin also increased the ratio of Bcl-X_L/Bax protein, and reduced intracellular ROS level, cytochrome c protein expression, cleaved caspase-9 protein expression, and cleaved caspase-3 protein expression. Additionally, di-*O*-demethylcurcumin treatment also reduced the expression of ER stress protein markers, including protein kinase RNA like endoplasmic reticulum kinase (PERK) phosphorylation, eukaryotic translation initiation factor 2 alpha (eIF2α) phosphorylation, inositol-requiring enzyme 1 (IRE1) phosphorylation, X-box-binding protein-1 (XBP-1), activating transcription factor (ATF6), C/EBP homologous protein (CHOP), and cleaved caspase-12 protein. CHOP and cleaved caspase-12 protein are the key mediators of apoptosis. Our data suggest that di-*O*-demethylcurcumin is a candidate protectant against neuronal death through its suppression of the apoptosis mediated by mitochondrial death and ER stress pathway.

1. Introduction

Alzheimer's disease (AD) is a progressive neurodegenerative disease of the central nervous system (CNS), affecting, generally, elderly people. AD is one of the most common forms of dementia, which is determined clinically by diagnosing for multiple cognitive deficits including memory loss, emotional disturbance, etc. (Hauptmann et al., 2006). The pathological hallmarks of AD are amyloid plaques and neurofibrillary tangles (NFT) (Hardy and Selkoe, 2002; Selkoe, 2001) that cause loss of neurons and synapses in the brain. Amyloid β (Aβ) is derived from the proteolytic cleavage of the amyloid precursor protein (APP) by β- and γ-secretase enzymes, and accumulate in the extracellular neuronal cells (Sisodia et al., 2001). NFT is accumulated within the neurons as a result of abnormal phosphorylation of the microtubules-associated tau-protein. Recent studies suggest that Aβ accumulation has been causatively implicated in the neuronal dysfunction and neuronal loss that underlie the clinical manifestations of AD (Dante et al., 2003). Furthermore, several lines of research have suggested that Aβ exerts neuronal toxicity through the production of reactive oxygen species (ROS) (Behl et al., 1994; Butterfield et al., 2007), which leads to neuronal apoptosis (Ramalingam and Kim, 2012) due to the involvement of the mitochondrial death pathway and the endoplasmic reticulum (ER) stress (Takuma et al., 2005). ER is an intracellular organelle

* Corresponding author. Department of Physiology, Faculty of Medicine, Chiang Mai University, Chiang Mai 50200, Thailand. Tel.: +66 53 945362; fax: +66 53 945365.
E-mail address: jtocharus@gmail.com (J. Tocharus).

http://dx.doi.org/10.1016/j.neuint.2014.10.008
0197-0186/

related to protein folding, intracellular calcium homeostasis, lipid synthesis, steroids and cholesterol. Cellular conditions in ER, such as depletion of calcium, alter glycosylation, and the oxidative stress leads to unfolded protein. Unfolded protein accumulation in ER lumen is termed as ER stress (Nakagawa et al., 2000); this accumulation activates unfolded protein response (UPR), thereby signaling responses for ER homeostasis by decreasing protein synthesis, and increasing chaperone and degradation (Schroder and Kaufman, 2005; Vembar and Brodsky, 2008). However, prolonged ER stress is associated with apoptotic cell death (Boyce and Yuan, 2006), which is caused by activating three signal transducers that are protein kinase RNA like endoplasmic reticulum kinase (PERK), activating transcription factor (ATF6) and inositol-requiring enzyme 1 (IRE1); then, upregulates the expression of the C/EBP homologous protein (CHOP) (Chen et al., 2012), caspase-12 protein (Nakagawa et al., 2000), and glucose related protein 78 (Grp78) (Kim et al., 2008). Moreover, apoptosis mainly involves excessive ROS-induced mitochondrial dysfunction upon the increase in the permeability of mitochondria membrane (Chen and Yan, 2007). These results in the inducing of proapoptotic protein such as Bax translocate from the cytoplasm to the mitochondria membrane and a decrease in the anti-apoptotic proteins (Bcl-2, Bcl-X_L). Thereafter, cytochrome c gets released to the cytoplasm and combines with apoptotic protease activating factor 1 (APAF-1) and procaspase-9 to become the active form of caspase-9 protein which stimulates the caspase-3 protein, and this leads to cell death (Li et al., 1997; Slee et al., 1999). Therefore, evidences suggest that suppression of Aβ-mediated neuronal apoptosis would be a target to attenuate progressive neuronal damages and provide a strategy for the given approach to the development and treatment of AD.

Curcumin is the major constituent of curcuminoids isolated from turmeric (*Curcuma longa* L.), with demethoxycurcumin and bisdemethoxycurcumin being the minor constituents. Previous studies have shown that curcumin has a wide range of beneficial properties, including antioxidant activity, anti-inflammatory activity, anticancer activity, neuroprotective effects, and antiviral activity (Bandgar et al., 2014; Belviranli et al., 2013; Bhullar et al., 2013; Morsy and El-Moselhy, 2013; Rath et al., 2013). Several groups of researchers are engaged in the design and synthesis of new curcuminoid analogs that exhibit higher physiological activities and pharmacological activities than the parent curcumin itself (Aroonrerk et al., 2012; Changtam et al., 2010; Sandur et al., 2007). Recently, we reported our research finding that di-*O*-demethylcurcumin, a chemically modified analog of curcumin, showed a potent anti-inflammatory activity greater than that of the parent curcumin (Tocharus et al., 2012). However, it remains unclear whether di-*O*-demethylcurcumin exerts neuroprotection against Aβ-induced neuronal damage. Considering the important role of Aβ in the pathogenesis of AD, elucidation of the effects of di-*O*-demethylcurcumin against Aβ-induced toxicity may provide a new insight into its potential application to the prevention or treatment of AD. It is, therefore, of interest to investigate whether di-*O*-demethylcurcumin would protect against Aβ-induced cytotoxicity in SK-N-SH cells. In the present study, we explored the possible mechanisms underlying the neuroprotective effects of di-*O*-demethylcurcumin against $A\beta_{25\text{-}35}$-induced apoptosis in SK-N-SH cells. We evaluated the protective effect of the production of ROS, and mitochondrial disruption, as well as ER stress.

2. Materials and methods

2.1. Materials

SK-N-SH cells (human neuroblastoma cells) were obtained from American Type Culture Collection (ATCC, Manassas, VA, USA). $A\beta_{25\text{-}35}$ was obtained from Sigma (St. Louis, MO, USA). Minimum essential medium (MEM), fetal bovine serum (FBS), penicillin, and streptomycin were purchased from GIBCO-BRL (Gaithersburg, MD, USA). The following antibodies were used for the western blot analysis: anti-Bcl-X_L, anti-Bax, anti-cytochrome c, anti-cleaved caspase-3, anti-cleaved caspase-9, anti-β-actin, anti-mouse IgG peroxidase-conjugated secondary antibody, anti-rabbit IgG peroxidase-conjugated secondary antibody (Millipore, Bedford, MA, USA), anti-Grp78, anti-CHOP, anti-PERK, anti-phospho-PERK, anti-phospho-eIF2α (Cell Signaling Technology, MA, USA), anti-ATF6, anti-XBP-1 (Santa Cruz Biotechnology, CA, USA), anti-phospho-IRE1α and anti-caspase-12 (Abcam, Cambridge, UK) and anti-β-actin.

2.2. Methods

$A\beta_{25\text{-}35}$ was dissolved in deionized distilled water at concentration of 1 mM and storage at –80 °C. Before it was used in each of the experiments, it was aggregated at 37 °C for a week, after which it was diluted to the required concentration with sterile water.

2.2.1. Cell culture

The SK-N-SH cells were cultured in MEM supplemented with 10% heat inactivated FBS, 100 units/ml penicillin, and 100 μg/ml streptomycin in humidified 95% air, at 37 °C and 5% CO_2 in an incubator. The cells were passaged by trypsinization every 2–3 days.

2.2.2. Preparation of di-O-demethylcurcumin

Curcumin (850 mg, 2.30 mmol), obtained from *Curcuma longa* as described previously (Changtam et al., 2010), was dissolved in dry CH_2Cl_2 (90 ml); the mixture was stirred at 0 °C or 5 min and BBr_3 (1 ml) was slowly added. The reaction mixture was stirred at 0 °C for 30 min and more BBr_3 (1 ml) was slowly added. After stirring at 0 °C for 1 h, water (200 ml) was added and the mixture was extracted with EtOAc. The combined organic phase was washed with water, dried over anhydrous Na_2SO_4 and the solvent was removed under vacuum. The crude products were separated by column chromatography using CH_2Cl_2-MeOH (10:1) as eluting solvent to yield mono-*O*-demethylcurcumin 240 mg (29%) and di-*O*-demethylcurcumin 450 mg (57%). The spectroscopic (^{1}H NMR and mass spectra) data were consistent with the reported values (Venkateswarlu et al., 2005).

2.2.3. Cell viability using MTS assay

The SK-N-SH cells were plated at a density of 2×10^5 cells/ml into 96 well plates (Corning Inc., Corning, NY, USA) and then incubated for 24 h at 37 °C in a CO_2 incubator. The cells were pretreated with di-*O*-demethylcurcumin (1 μM, 2 μM, 4 μM and 8 μM) for 2 h, which was followed by the addition of 10 μM $A\beta_{25\text{-}35}$ for 24 h. Thereafter, PrestoBlue reagent was added to each well and incubated additionally for 2 h at 37 °C under a humidified condition of 5% CO_2. The absorbance was measured using a microplate reader (Bio-Tek, Instruments, Winoaski, VT, USA) at the wavelength of 540 nm from three independent experiments. The background absorbance was measured at 600 nm and subtracted.

2.2.4. Determination of intracellular ROS by DCF assay

The cells at a density of 2×10^4 cells/well were plated in 96 well plates and then incubated for 24 h at 37 °C in CO_2 incubator. The cells were pretreated with di-*O*-demethylcurcumin (2 μM, 4 μM and 8 μM) for 2 h, and then treated with $A\beta_{25\text{-}35}$ for 24 h. The medium was removed, and DCFH-DA solutions were added for 25 min. The absorbance was measured using a fluorescence microplate reader (DTX800, Beckman Coulter, Austria) at an excitation wavelength of

485 nm and an emission wavelength of 535 nm. Fluorescent images were observed and collected by a fluorescence microscope from three independent experiments (Olympus AX-70, Olympus, Tokyo, Japan).

2.2.5. Cell apoptosis analysis

The cell death was investigated using fluorescein isothiocyanate (FITC) annexin V apoptosis detection kit (BD Bioscience, Canada) by following the manufacturer's instructions. Briefly, the SK-N-SH cells were plated at a density of 5×10^5 cells/well in six well plate and pretreated with di-*O*-demethylcurcumin for 2 h, which was followed by treatment in the presence or absence of $A\beta_{25\text{-}35}$ for 24 h; thereafter, the cells were collected and resuspended in 1 × binding buffer and incubated with annexin V-FITC and propidium iodide for 15 min in the dark. The cells were analyzed using FACS canto ii flow cytometry. The percentage of the apoptotic cells from three independent experiments was calculated using Diva software (FAC BIVA).

2.2.6. Assessment of nuclear morphological change

For the assessment of the nuclear morphological change of the apoptotic cells in the SK-N-SH cells, the cells were plated at a density of 2×10^4 cells/well in six well plates. The cells were pretreated with di-*O*-demethycurcumin for 2 h, and then treated in the presence or absence of $A\beta_{25\text{-}35}$ for 24 h; the cells were then fixed with 2.5% glutaraldehyde in phosphate buffer saline (PBS), pH 7.4 at 4 °C until embedding. Thereafter, the cells were post-fixed with 1% osmium tetroxide for 2 h. Following this, they were dehydrated in a graded series (20–100%) of ethanol, and then embedded in araldite. Ultrathin sections were cut on an ultra microtome, using diamond knives collected on copper grids, and stained with 4% uranyl acetate and Reynolds lead citrate. The images from three independent experiments were detected with the help of an electron microscope (JEM-2200 FS; JEOL, Tokyo, Japan).

2.2.7. Western blot

The SK-N-SH cells were cultured in a density of 5×10^5 cells/ml in a 60 mm culture dish, at 37 °C, overnight. The cells were pretreated with di-*O*-demethylcurcumin at concentrations of 2 μM, 4 μM and 8 μM for 2 h in the presence or absence of $A\beta_{25\text{-}35}$ and lysed in a lysis buffer containing NP-40, 1% sodium deoxycholate, 0.1% sodium dodecyl sulfate, 40 mM β-glycerophosphate, 50 mM sodium fluoride, 2 mM sodium orthovanadate and 1× protease inhibitors at 4 °C for 15 min. The protein concentration was determined using the Bradford protein assay (Bio-Rad Laboratories, Hercules, CA, USA) and equal amounts of proteins were electrophoresed in a 10–15% SDS polyacrylamide gel and then transferred to a polyvinylidene fluoride (PVDF) membrane (Immobilon-P, Millipore, Bedford, MA, USA) at 400 mA for 30 min. Thereafter, it was incubated with the indicated antibodies (anti-p-PERK, anti-PERK, anti-ATF6, anti-Grp78, anti-p-eIF2α, anti-eIF2α, anti-CHOP, anti-IRE1, anti-p-IRE1, anti-cleaved caspase 12, anti-XBP-1, anti-Bax, anti-Bcl-X_L, anti-cytochrome c, anti-cleaved caspase-3 protein and anti-cleaved caspase-9 protein) in 1:1000–1:2000 dilution with phosphate-buffered saline with Tween 20 (PBST) at 4 °C, overnight. The blots were incubated with horseradish peroxidase-conjugated secondary antibodies for 1 h at room temperature. The signal was visualized as blots using the Immobilon Western (Millipore, MA, USA) and exposed to an X-ray film. The densitometry from three independent experiments was analyzed using the Image-J® software.

2.3. Statistical analysis

All the data are represented as the mean ± SD. Statistical significance was determined using one-way ANOVA, followed by Post Hoc Dunnett's test. Values of $P < 0.001$, $P < 0.01$, $P < 0.05$ were considered as statistically significant.

3. Results

3.1. Di-O-demethylcurcumin increases cell viability against $A\beta_{25\text{-}35}$

The cells were pretreated with di-*O*-demethylcurcumin (2 μM, 4 μM and 8 μM) for 2 h prior to the addition of 10 μM of $A\beta_{25\text{-}35}$, and the protective effect was determined after 24 h of treatment. The result showed that 10 μM of $A\beta_{25\text{-}35}$ induced significantly the cell death of approximately 30% of the cells ($P < 0.05$) compared to the control group (Fig. 1). Di-*O*-demethylcurcumin attenuated the cytotoxicity of $A\beta_{25\text{-}35}$ and significantly increased ($P < 0.001$) the cell viability in a concentration-dependent manner. The cell viability upon pretreatment with di-*O*-demethycurcumin at concentrations of 2 μM, 4 μM and 8 μM for 2 h before being treated with $A\beta_{25\text{-}35}$ for 24 h were 84.31 ± 1.07%, 88.96 ± 1.30%, and 93.24 ± 2.30%, respectively. At these concentrations, di-*O*-demethylcurcumin alone did not show any obvious effects on the viability of the SK-N-SH cells (Fig. 1).

3.2. Di-O-demethylcurcumin attenuated $A\beta_{25\text{-}35}$ induced production of ROS in SK-N-SH cells

An investigation was carried out to examine whether di-*O*-demethylcurcumin could inhibit the ROS generation induced by $A\beta_{25\text{-}35}$. We determined the effects of di-*O*-demethylcurcumin on ROS production by measuring the redox-sensitive dye DCFH-DA. As demonstrated in Fig. 2A,B, exposure to 10 μM of $A\beta_{25\text{-}35}$ of the SK-N-SH cells for 24 h resulted in a significant increase in the amount of ROS, by 238.44 ± 10.67%, as compared to the control group. After the pretreatment with 2 μM, 4 μM and 8 μM of di-*O*-demethylcurcumin in SK-N-SH cells before being treated with $A\beta_{25\text{-}35}$, the ROS levels were found to have significantly decreased ($P < 0.001$) in comparison with the $A\beta_{25\text{-}35}$-treated SK-N-SH group. At these concentrations, it was observed that di-*O*-demethylcurcumin alone did not show any

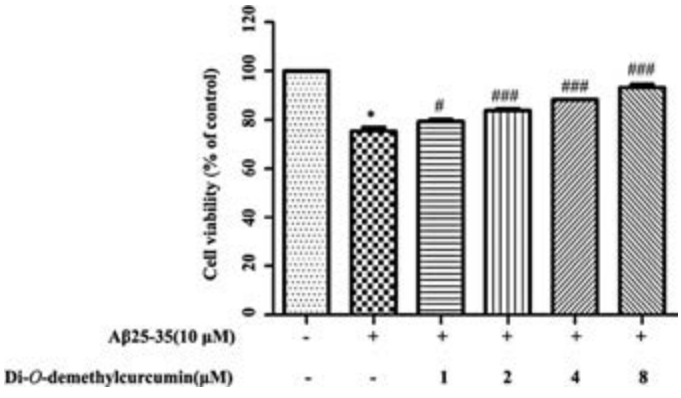

Fig. 1. Di-*O*-demethylcurcumin improves the cell viability of the SK-N-SH cells-induced by $A\beta_{25\text{-}35}$. The SK-N-SH cells were pretreated with various concentrations (2–8 μM) of di-*O*-demethylcurcumin for 2 h, which was followed by treatment with 10 μM $A\beta_{25\text{-}35}$ for 24 h. The cell viability was measured using the 3-(4,5-dimethylthiazol-2-yl)-5-(3-carboxymethoxyphenyl)-2-(4-sulfophenyl)-2H-tetrazolium (MTS) assay. The data were normalized by using a control group. The values are presented as mean percent of control ± SD of three independent experiments. $^{*}P < 0.05$ vs. control group; $^{\#}P < 0.05$, $^{\#\#\#}P < 0.001$ vs. group treated with $A\beta_{25\text{-}35}$ alone.

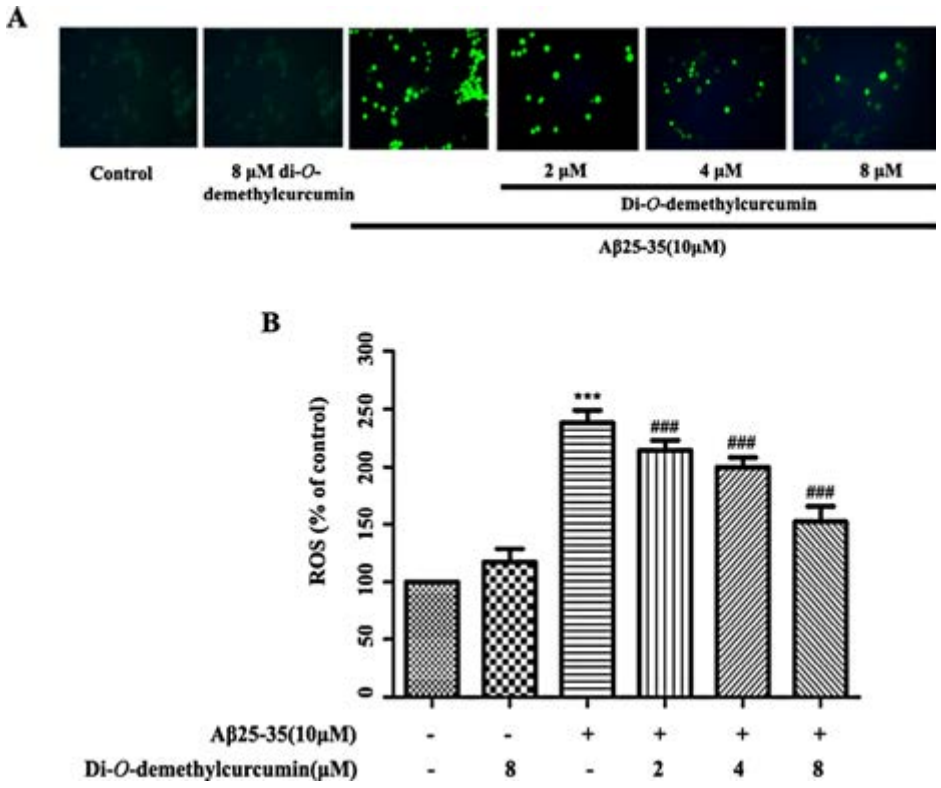

Fig. 2. The effect of di-*O*-demethylcurcumin on $A\beta_{25\text{-}35}$-induced ROS production in SK-N-SH cells. **A:** Scanning Confocal Microscopy detected $A\beta_{25\text{-}35}$-induced ROS production in SK-N-SH cells. a: The control group. b: The SK-N-SH cells treated with di-*O*-demethylcurcumin alone. c: The SK-N-SH cells treated with 10 μM of $A\beta_{25\text{-}35}$ alone. d–f: SK-N-SH cells pretreated with di-*O*-demethylcurcumin at the concentration of 2 μM, 4 μM and 8 μM for 2 h prior to treatment with 10 μM $A\beta_{25\text{-}35}$ for 24 h. **B:** The values of ROS are presented as the mean percent of control ± SD of three independent experiments. $^{***}P < 0.001$ vs. control group; $^{###}P < 0.001$ vs. group treated with $A\beta_{25\text{-}35}$ alone.

obvious effects on the basal level of ROS (Fig. 2A,B). These results imply that di-*O*-demethylcurcumin has free radical scavenging effect in SK-N-SH cells activated by $A\beta_{25\text{-}35}$.

3.3. *Di*-O-*demethylcurcumin prevents cell apoptosis caused by* $A\beta_{25\text{-}35}$

In order to confirm the protective effect of di-*O*-demethylcurcumin against $A\beta_{25\text{-}35}$-induced SK-N-SH cells death, we investigated the nuclear morphological change in the apoptotic cells by using transmission electron microscope (TEM). As illustrated in Fig. 3A, $A\beta_{25\text{-}35}$ treatment alone showed nuclear condensation and cell shrinkage compared to the control. On the other hand, treatment with di-*O*-demethylcurcumin was found to decrease the apoptotic morphological change, and the morphology was observed to be similar to that of the control group. In addition, the number of apoptotic cells was also quantitatively analyzed using flow cytometry with Annexin V-FITC/PI double staining. The $A\beta_{25\text{-}35}$-treated cells significantly increased ($P < 0.001$) the number of apoptotic cells as compared to the control group. However, pretreatment with di-*O*-demethylcurcumin was observed to significantly reduce ($P < 0.001$) the number of apoptotic cells as compared to the cells treated with the $A\beta_{25\text{-}35}$ group in a dose-dependent manner (Fig. 3B,C). The apoptotic cells at the time of pretreatment with di-*O*-demethylcurcumin (at concentrations of 2 μM, 4 μM and 8 μM) were 62.60 ± 2.35%, 38.73 ± 1.35%, and 14.77 ± 1.63%, respectively. These results suggest that di-*O*-demethylcurcumin suppresses $A\beta_{25\text{-}35}$-induced cell apoptosis in SK-N-SH cells.

3.4. *Effects of di*-O-*demethylcurcumin on* $A\beta_{25\text{-}35}$*-induced ER stress in SK-N-SH cells*

To investigate whether di-*O*-demethylcurcumin could suppress the apoptosis mediated by the ER stress pathway, we first determined whether $A\beta_{25\text{-}35}$ could induce ER stress. With this purpose, we investigated the expression of Grp78, a marker of ER stress in SK-N-SH cells. The SK-N-SH cells were treated with 10 μM of $A\beta_{25\text{-}35}$ for 0 h, 3 h, 6 h, 9 h, 12 h and 24 h, following which the cells were harvested. The results revealed that $A\beta_{25\text{-}35}$ had significantly increased the expression of the Grp78 proteins in the SK-N-SH cells ($P < 0.001$), with the maximum level being observed at the 12th h. Thereafter, we investigated the expression of the three major sensors of the ER stress pathway, including PERK, IRE1 and ATF6, using the western blot analysis. The activation of the PERK signal pathway was determined using the phosphorylated form of eIF2α and PERK in the SK-N-SH cells was treated with $A\beta_{25\text{-}35}$. The presence of $A\beta_{25\text{-}35}$ increased the phosphorylated form of eIF2α and the PERK proteins in a time-dependent manner, with the maximum level being observed at the 12th h in the SK-N-SH cells (Fig. 4A). Next, we investigated the effects of $A\beta_{25\text{-}35}$ activation on the IRE1 signal pathway, which was found out by determining the expression levels of XBP-1 and the phosphorylation form of p-IRE1 using the western blotting analysis. It was observed that $A\beta_{25\text{-}35}$ had increased the expression of phosphorylated IRE1 in a time-dependent manner (Fig. 4A). As XBP-1 mRNA is a specific substrate of IRE1, the splicing of XBP-1 is commonly used as a marker for IRE1 activation. We determined the activation of IRE1 by detecting the XBP-1 protein in the SK-N-SH cells. It was found that $A\beta_{25\text{-}35}$ had significantly

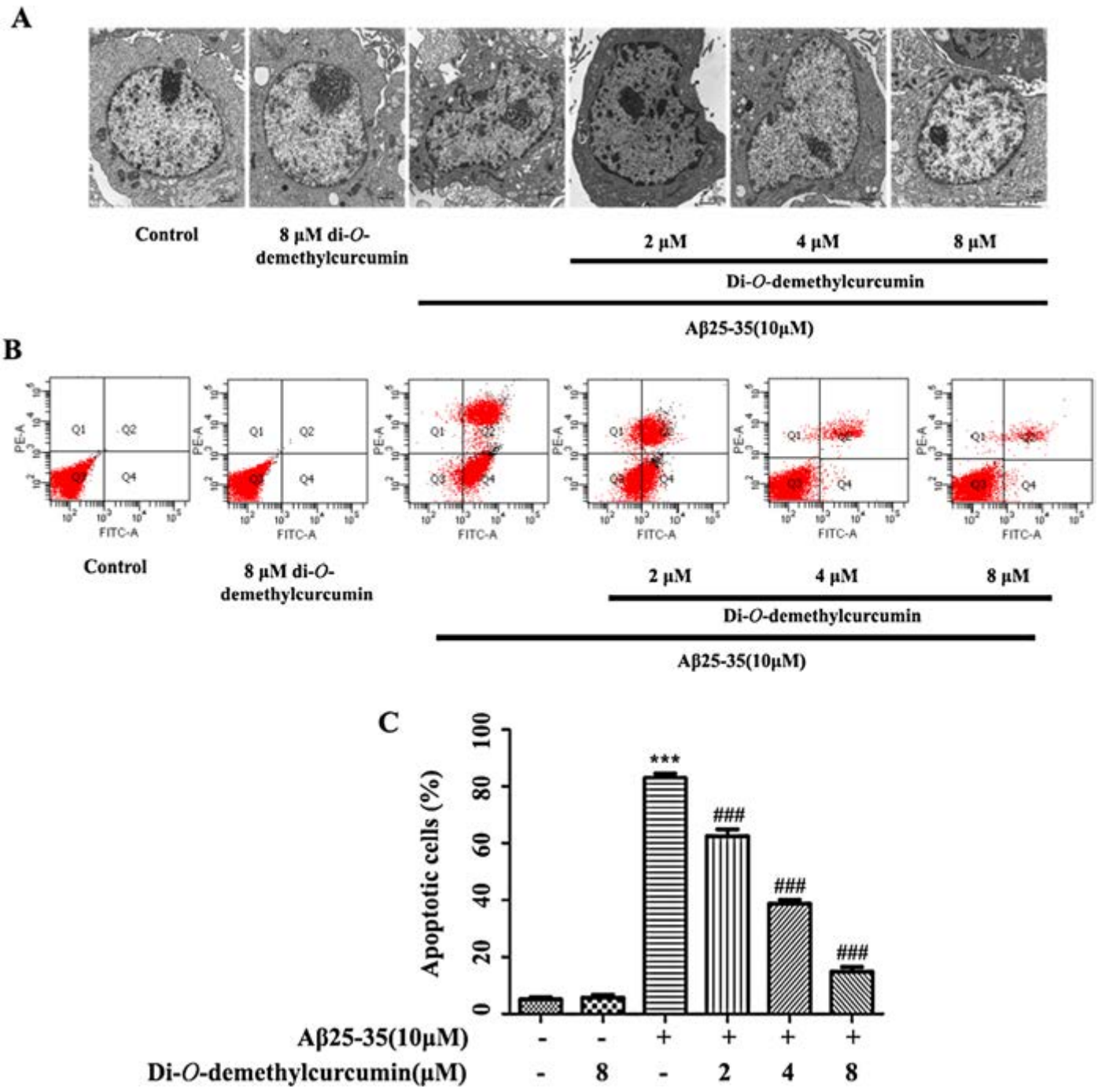

Fig. 3. Di-*O*-demethylcurcumin attenuated $A\beta_{25\text{-}35}$-induced apoptosis in SK-N-SH cells. **A:** The morphological changes of SK-N-SH cells were detected using TEM. The effect of di-*O*-demethylcurcumin on $A\beta_{25\text{-}35}$ induced apoptosis in SK-N-SH cells. a: The control group. b: The SK-N-SH cells treated with di-*O*-demethylcurcumin alone. c: SK-N-SH cells treated with 10 μM of $A\beta_{25\text{-}35}$ alone. d–f: SK-N-SH cells pretreated with di-*O*-demethylcurcumin at the concentration of 2 μM, 4 μM and 8 μM for 2 h prior to treatment with 10 μM of $A\beta_{25\text{-}35}$ for 24 h. **B:** SK-N-SH cells were labeled with Annexin V-FITC and PI. The apoptotic SK-N-SH cells were analyzed using flow cytometry. The numbers indicate the percentage of the cells in each quadrant (lower left: $FITC^-/PI^-$, intact cells; lower right:$FITC^+/PI^-$, apoptotic cells; upper left: $FITC^-/PI^+$, necrotic cells; upper right: $FITC^+/PI^+$, late apoptotic cells). **C:** The percentage of apoptotic cells are presented as the mean percent of control ± SD of three independent experiments. $^{***}P < 0.001$ vs. control group; $^{\#\#\#}P < 0.001$ vs. group treated with $A\beta_{25\text{-}35}$ alone.

increased ($P < 0.001$) the XBP-1 protein in response to the exposed time in a time-dependent manner, with the maximum increase observed at the 24th h (Fig. 4A). In addition, we investigated the expression of the ER stress proteins of ATF6, CHOP and cleaved caspase 12 using the western blotting analysis, and showed that the optimal time expressions of these three are at the 12th h, 24th h and 9th h, respectively, after being exposed to $A\beta_{25\text{-}35}$ (Fig. 4A). Altogether, the result suggested that the expression of the ER stress proteins increased in a time-dependent manner, with the maximum level being observed between the 9th h and 24th h in the SK-N-SH cells treated with $A\beta_{25\text{-}35}$. Based on these results, the investigation for the determination of the further effects of di-*O*-demethylcurcumin in $A\beta_{25\text{-}35}$-induced ER stress was subsequently carried out at this time point. In order to determine the cytoprotective effect of di-*O*-demethylcurcumin in $A\beta_{25\text{-}35}$-induced ER stress, the SK-N-SH cells were pretreated with various concentrations of

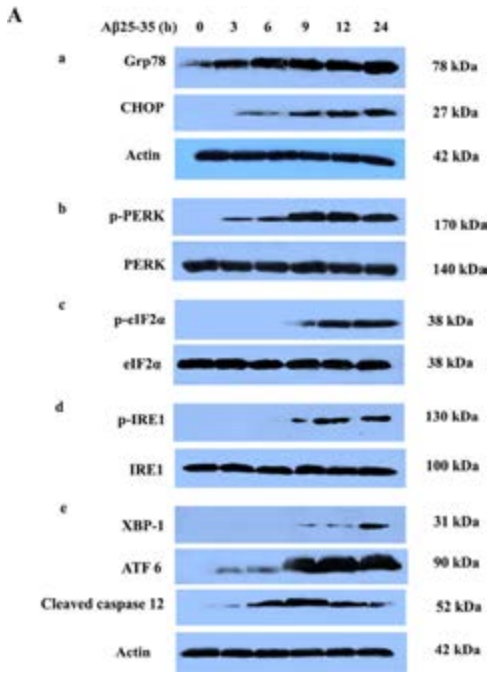

Fig. 4. Di-*O*-demethylcurcumin suppresses $A\beta_{25-35}$-induced ER stress in SK-N-SH cells. **A:** SK-N-SH cells were treated with 10 μM $A\beta_{25-35}$ for 0 h, 3 h, 6 h, 9 h, 12 h, and 24 h. The expression of Grp78, p-PERK, PERK, p-eIF2α, eIF2α, p-IRE1, IRE1, XBP-1, ATF6, CHOP, cleaved caspase 12 protein were examined using the western blot analysis. The β-actin antibody was used as an internal control. **B:** A representative western blot showing the expression of p-PERK, PERK, p-eIF2α, eIF2α, p-IRE1, IRE1 and XBP-1 in SK-N-SH cells. The cells were pretreated with di-*O*-demethylcurcumin (at concentrations of 2 μM, 4 μM and 8 μM) for 2 h, which was followed by treatment with 10 μM of $A\beta_{25-35}$ for 24 h. a: The quantitative analysis of p-PERK was normalized to the PERK. b: The quantitative analysis of p-eIF2α was normalized to the eIF2α. c: The quantitative analysis of p-IRE1 was normalized to the IRE1. d: The quantitative analysis of XBP-1 was normalized to β-actin. **C:** A representative western blot showing the expression of Grp78, ATF6 and CHOP in SK-N-SH cells. The cells were pretreated with di-*O*-demethylcurcumin (at concentrations of 2 μM, 4 μM and 8 μM) for 2 h, which was followed by treatment with 10 μM $A\beta_{25-35}$ for 24 h. a: The quantitative analysis of Grp78 was normalized to the β-actin. b: The quantitative analysis of CHOP was normalized to the β-actin. c: The quantitative analysis of the cleaved caspase-12 protein was normalized to β-actin. The values are presented as mean ± SD of three independent experiments. $^{***}P < 0.001$ vs. control group; $^{\#}P < 0.05$, $^{\#\#}P < 0.01$, $^{\#\#\#}P < 0.001$ vs. group treated with $A\beta_{25-35}$ alone.

di-*O*-demethylcurcumin (2 μM, 4 μM and 8 μM) for 2 h, prior to $A\beta_{25-35}$ activation. The expressions of the phosphorylated forms of eIF2α, PERK, IRE1, and the expression of XBP-1, ATF6, CHOP, cleaved caspase-12 protein and Grp78, were observed to have significantly decreased ($P < 0.001$) in a concentration-dependent manner (Fig. 4B,C). These data suggest that di-*O*-demethylcurcumin attenuated apoptosis through the ER stress pathway in SK-N-SH cells.

3.5. *Effects of di-O-demethylcurcumin on Aβ$_{25-35}$-induced mitochondria apoptosis pathway in SK-N-SH cells*

An analysis was conducted to determine the protective effect of di-*O*-demethylcurcumin against $A\beta_{25-35}$-induced mitochondrial death pathway in SK-N-SH cells. We investigated the expression of Bcl-X_L, Bax, cytochrome c, cleaved caspase-9 protein, and cleaved caspase-3 proteins at 0 h, 3 h, 6 h, 9 h, 12 h and 24 h in SK-N-SH cells activated using 10 μM of $A\beta_{25-35}$. As presented in Fig. 5A, the expression of Bcl-X_L was found to have significantly decreased in a time-dependent manner ($P < 0.001$). On the other hand, the expression of Bax was observed to have significantly increased in a time-dependent manner ($P < 0.001$). The release of cytochrome c to cytosol was also found to have significantly increased ($P < 0.001$) in a time-dependent manner, with the maximum level being observed at the 12th h in the SK-N-SH cells activated by $A\beta_{25-35}$. Next, we carried out an investigation to confirm that the relevant mitochondria apoptosis pathway was affected by the overexpression of the cleaved caspase-9 protein and the cleaved caspase-3 protein, which shows the presence of the apoptosis cells. We found that both the cleaved caspase-9 protein and the cleaved caspase-3 protein had the optimal time of expression at the 24th h after the treatment with 10 μM of $A\beta_{25-35}$ (Fig. 5A). Pretreatment with various concentration of di-*O*-demethylcurcumin for 2 h prior to the treatment with 10 μM of $A\beta_{25-35}$ was found to significantly increase ($P < 0.001$) the Bcl-X_L/Bax ratio in a concentration-dependent manner (Fig. 5B,C). In addition, it was observed that di-*O*-demethylcurcumin also markedly decreased ($P < 0.001$) the expression of cytochrome c, cleaved caspase-9 protein, and cleaved caspase-3 protein in a concentration-dependent manner (Fig. 5D,E,F).

4. Discussion

It is now well known that Aβ is neurotoxic and contributes to the pathogenesis of AD. The toxicity of Aβ is associated with senile plagues formed in AD brains, which is attributable to the amino acid located in position 25–35 of the full length length, containing the functional domain that is involved in the neurotoxic effects in AD (Kubo et al., 2002; Millucci et al., 2010). The $A\beta_{25-35}$ is widely used to as an experimental model of AD, thus, we implied that cultured SK-N-SH cells treated with $A\beta_{25-35}$ as used in the present study would provide a suitable approach to determine the effects of di-*O*-demethylcurcumin on Aβ toxicity. Previous studies have reported that Aβ induces oxidative stress by producing excessive amount of ROS (Shearman et al., 1994), which lead to cell membrane lipid destruction, DNA damage, oxidation of proteins, and, finally, apoptosis (Zawia et al., 2009). Thus, suppression of oxidative stress brings with it the benefit of preventing AD (Calabrese et al., 2008). Di-*O*-demethylcurcumin, a demethylated analog of curcumin, has been reported to be a strong anti-inflammatory agent greater than its parent compound, as demonstrated in our previous study (Tocharus et al., 2012). In this study, we further investigated the protective role of di-*O*-demethylcurcumin against $A\beta_{25-35}$-induced apoptosis mediated by mitochondrial death pathway and

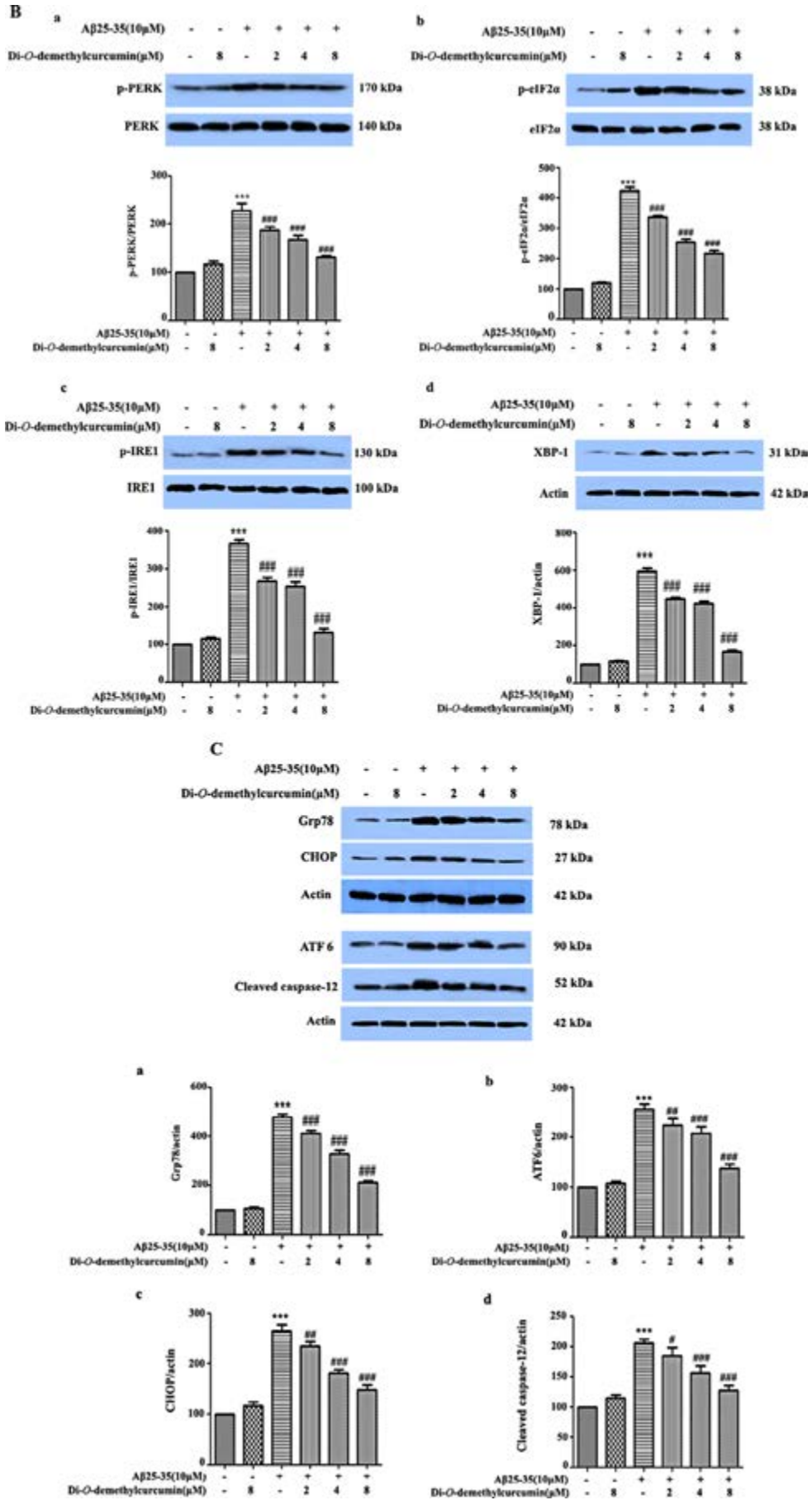

Fig. 4. (*continued*)

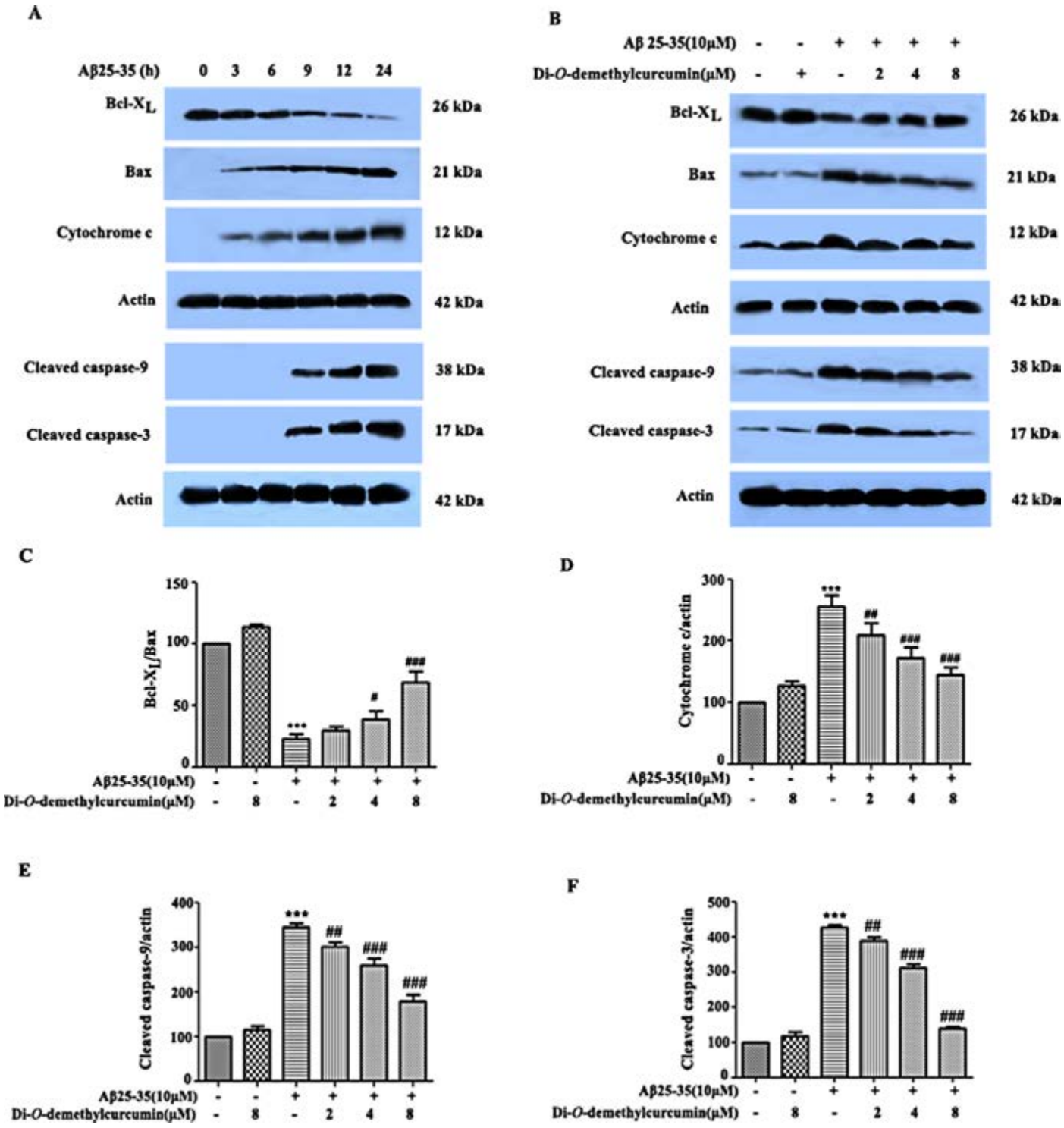

Fig. 5. The effects of di-*O*-demethylcurcumin on $A\beta_{25\text{-}35}$-induced mitochondria apoptosis pathway in SK-N-SH cells. **A:** A representative western blot showing the expression of Bcl-X_L, Bax, cytochrome c, the cleaved caspase-9 protein and the cleaved caspase-3 protein. The SK-N-SH cells were treated with 10 μM $A\beta_{25\text{-}35}$ for 0 h, 3 h, 6 h, 9 h, 12 h, and 24 h. The β-actin antibody was used as an internal control. **B:** A representative western blot showing the expression of Bcl-X_L, Bax, cytochrome c, cleaved caspase-9 and cleaved caspase-3 protein in the SK-N-SH cells. The cells were pretreated with di-*O*-demethylcurcumin (at concentrations of 2 μM, 4 μM and 8 μM) for 2 h, which was followed by treatment with 10 μM of $A\beta_{25\text{-}35}$ for 24 h. **C:** The quantitative analysis of Bcl-X_L was normalized to the Bax. **D:** The quantitative analysis of cytochrome c was normalized to β-actin. **E:** The quantitative analysis of the cleaved caspase-9 protein was normalized to β-actin. **F:** The quantitative analysis of cleaved caspase-3 protein was normalized to β-actin. The values are presented as mean ± SD of three independent experiments. $^{***}P < 0.001$ vs. control group; $^{\#}P < 0.05$, $^{\#\#}P < 0.01$, $^{\#\#\#}P < 0.001$ vs. group treated with $A\beta_{25\text{-}35}$ alone.

ER stress pathway. We first investigated $A\beta_{25\text{-}35}$-induced cytotoxicity in SK-N-SH cells using the MTS assay. It was observed that pretreatment with various concentrations of di-*O*-demethylcurcumin had markedly increased the cell viability in a concentration-dependent manner. We next explored if di-*O*-demethylcurcumin has protective effects against $A\beta_{25\text{-}35}$-induced neuronal cell apoptosis. $A\beta_{25\text{-}35}$-treated cells were investigated using TEM, and the results of the investigation revealed typical morphological

features of apoptosis with chromatin condensation and nucleus fragmentation. We next carried out the quantitative analysis for the number of apoptotic cells using flow cytometry. The results showed that di-*O*-demethylcurcumin can protect SK-N-SH cells against Aβ-induced apoptosis. Simultaneously, we found out that $A\beta_{25\text{-}35}$ is able to induce mitochondrial dysfunction (Costa et al., 2012) as determined by its ability to increase ROS accumulation, whereas di-*O*-demethylcurcumin has the ability to reverse these events. A large number of experiments have demonstrated that $A\beta_{25\text{-}35}$ plays an important role in cell apoptosis mediated by mitochondrial death pathway and ER stress pathway (Alberdi et al., 2013; Costa et al., 2012; Takuma et al., 2005). It is well known that $A\beta_{25\text{-}35}$ induces mitochondria dysfunction by increasing the intracellular ROS production (Shearman et al., 1994), depolarizing the mitochondrial membrane, opening the mitochondrial permeability transition pore (MPTP), and inducing the release of cytochrome c, which, in turn, activates caspase-3 protein which plays an important role in cell apoptosis (Budihardjo et al., 1999; Manczak et al., 2010; Zhang and Armstrong, 2007). Our findings are consistent with previous reports showing that treatment with $A\beta_{25\text{-}35}$ induced mitochondrial dysfunction by increasing free radicals and reducing the mitochondrial membrane potential, thereby upregulating cytochrome c, caspase-9 protein and caspase-3 protein and downregulating the ratio of Bcl-X_L/Bax, and also that di-*O*-demethylcurcumin suppressed this activation (Budihardjo et al., 1999; Manczak et al., 2010; Zhang and Armstrong, 2007). Accumulations of ROS can result in oxidative stress, impairment of cell function, and apoptosis. It is a widely accepted fact that long periods of accumulation of unfolded protein in ER corresponds to apoptosis in AD (Boyce and Yuan, 2006). We therefore investigated the molecular events associated with $A\beta_{25\text{-}35}$-induced ER stress (Ferreiro et al., 2006). ER plays an important role in protein folding and modification. Protein biosynthesis in ER can be interfered with because of a variety of toxic conditions, including hypoxia, nutrient deprivation, Ca^{2+} overload, etc., which initiate the unfold protein response (UPR) that causes ER stress. ER stress triggers several specific signaling pathways, such as ER-associated protein degradation and UPR (Hoozemans et al., 2005). UPR is initiated by three ER-resident transmembrane proteins known as sensors of ER stress (Ron and Walter, 2007), namely, PERK, ATF6 and IRE1, which are activated by the ER-resident chaperone glucose-regulated protein of 78 kDa (Grp78 or BiP) (Calfon et al., 2002; Kim et al., 2008). This study provides evidence that $A\beta_{25\text{-}35}$ activates ER stress signaling pathways in SK-N-SH cells, and that the induction of ER stress is implicated in $A\beta_{25\text{-}35}$-induced apoptosis. We demonstrated that $A\beta_{25\text{-}35}$ induced the up-regulation of Grp78, p-PERK, p-eIF2α, and cleaved ATF6α, and increased the expression of CHOP and the caspase-12 protein which are important apoptotic inducers. All the same, it was also demonstrated that pretreatment with di-*O*-demethylcurcumin suppressed the activation of ER stress signaling pathway by inhibiting the Grp78, p-PERK, p-eIF2α, and cleaved ATF6α, and also decreased the expression of CHOP and the caspase-12 protein. A number of studies have demonstrated that prolonged activation of ER stress can activate the expression of CHOP and the caspase-12 protein, the key mediators of ER stress-induced cell death pathways in AD (Chen et al., 2012; Paschen and Mengesdorf, 2005). CHOP, a transcription factor induced by ATF6, PERK or IRE1, regulates cell death by suppressing the expression of the Bcl-2 protein (Hacki et al., 2000; McCullough et al., 2001) as well as by increasing the Bax protein (Gotoh et al., 2004; Paradis et al., 1996). Additionally, caspase-12 protein is an ER stress specific protein which activates the caspase-9 protein (Ishige et al., 2007; Morishima et al., 2002), a process that would lead to the activation of the caspase-3 pathways during apoptosis in AD. Thus, this study confirms that increased levels of CHOP and caspase-12 protein in neuronal cells leads to ER-stress-associated apoptosis. Therefore, di-*O*-demethylcurcumin-mediated inhibition of the CHOP and caspase-12 expression may be a key strategy in the efforts toward preventing ER stress-induced effects by $A\beta_{25\text{-}35}$.

In conclusion, it can be stated that the results here show that $A\beta_{25\text{-}35}$-treated SK-N-SH cells undergo apoptosis and di-*O*-demethylcurcumin exerts neuroprotective, antioxidative and anti-apoptotic effects by attenuating the mitochondrial death pathway and the ER stress pathway. Thus, the protective effects of di-*O*-demethylcurcumin against neuronal neurotoxins may help to provide the pharmacological basis of its clinical usage in the prevention or palliation of neurodegeneration in AD.

Acknowledgments

This work was supported by the Faculty of Medicine Research Fund, Chiang Mai University (grant no. 72/2557), and the Graduate School, Chiang Mai University, Chiang Mai, Thailand. Partial supports from The Thailand Research Fund (grant no. DBG5680006) and the Center of Excellence for Innovation in Chemistry, Office of the Higher Education Commission, are gratefully acknowledged.

References

Alberdi, E., Wyssenbach, A., Alberdi, M., Sanchez-Gomez, M.V., Cavaliere, F., Rodriguez, J.J., et al., 2013. Ca(2+)-dependent endoplasmic reticulum stress correlates with astrogliosis in oligomeric amyloid beta-treated astrocytes and in a model of Alzheimer's disease. Aging Cell 12, 292–302.

Aroonrerk, N., Changtam, C., Kirtikara, K., Suksamrarn, A., 2012. Inhibitory effects of di-*O*-demethylcurcumin on interleukin-1B-induced interleukin-6 production from human gingival fibroblasts. J. Dent. Sci. 7, 350–358.

Bandgar, B.P., Kinkar, S.N., Chavan, H.V., Jalde, S.S., Shaikh, R.U., Gacche, R.N., 2014. Synthesis and biological evaluation of asymmetric indole curcumin analogs as potential anti-inflammatory and antioxidant agents. J. Enzyme Inhib. Med. Chem. 29, 7–11.

Behl, C., Davis, J.B., Lesley, R., Schubert, D., 1994. Hydrogen peroxide mediates amyloid beta protein toxicity. Cell 77, 817–827.

Belviranli, M., Okudan, N., Atalik, K.E., Oz, M., 2013. Curcumin improves spatial memory and decreases oxidative damage in aged female rats. Biogerontology 14, 187–196.

Bhullar, K.S., Jha, A., Youssef, D., Rupasinghe, H.P., 2013. Curcumin and its carbocyclic analogs: structure-activity in relation to antioxidant and selected biological properties. Molecules 18, 5389–5404.

Boyce, M., Yuan, J., 2006. Cellular response to endoplasmic reticulum stress: a matter of life or death. Cell Death Differ. 13, 363–373.

Budihardjo, I., Oliver, H., Lutter, M., Luo, X., Wang, X., 1999. Biochemical pathways of caspase activation during apoptosis. Annu. Rev. Cell Dev. Biol. 15, 269–290.

Butterfield, D.A., Reed, T., Newman, S.F., Sultana, R., 2007. Roles of amyloid beta-peptide-associated oxidative stress and brain protein modifications in the pathogenesis of Alzheimer's disease and mild cognitive impairment. Free Radic. Biol. Med. 43, 658–677.

Calabrese, V., Cornelius, C., Mancuso, C., Pennisi, G., Calafato, S., Bellia, F., et al., 2008. Cellular stress response: a novel target for chemoprevention and nutritional neuroprotection in aging, neurodegenerative disorders and longevity. Neurochem. Res. 33, 2444–2471.

Calfon, M., Zeng, H., Urano, F., Till, J.H., Hubbard, S.R., Harding, H.P., et al., 2002. IRE1 couples endoplasmic reticulum load to secretory capacity by processing the XBP-1 mRNA. Nature 415, 92–96.

Changtam, C., de Koning, H.P., Ibrahim, H., Sajid, M.S., Gould, M.K., Suksamrarn, A., 2010. Curcuminoid analogs with potent activity against Trypanosoma and Leishmania species. Eur. J. Med. Chem. 45, 941–956.

Chen, C.M., Wu, C.T., Chiang, C.K., Liao, B.W., Liu, S.H., 2012. C/EBP homologous protein (CHOP) deficiency aggravates hippocampal cell apoptosis and impairs memory performance. PLoS ONE 7, e40801.

Chen, J.X., Yan, S.D., 2007. Amyloid-beta-induced mitochondrial dysfunction. J. Alzheimers Dis. 12, 177–184.

Costa, R.O., Ferreiro, E., Martins, I., Santana, I., Cardoso, S.M., Oliveira, C.R., et al., 2012. Amyloid beta-induced ER stress is enhanced under mitochondrial dysfunction conditions. Neurobiol. Aging 33, 824.e5–e16.

Dante, S., Hauss, T., Dencher, N.A., 2003. Insertion of externally administered amyloid beta peptide 25-35 and perturbation of lipid bilayers. Biochemistry 42, 13667–13672.

Ferreiro, E., Resende, R., Costa, R., Oliveira, C.R., Pereira, C.M., 2006. An endoplasmic-reticulum-specific apoptotic pathway is involved in prion and amyloid-beta peptides neurotoxicity. Neurobiol. Dis. 23, 669–678.

Gotoh, T., Terada, K., Oyadomari, S., Mori, M., 2004. Hsp70-DnaJ chaperone pair prevents nitric oxide- and CHOP-induced apoptosis by inhibiting translocation of Bax to mitochondria. Cell Death Differ. 11, 390–402.

Hacki, J., Egger, L., Monney, L., Conus, S., Rosse, T., Fellay, I., et al., 2000. Apoptotic crosstalk between the endoplasmic reticulum and mitochondria controlled by Bcl-2. Oncogene 19, 2286–2295.
Hardy, J., Selkoe, D.J., 2002. The amyloid hypothesis of Alzheimer's disease: progress and problems on the road to therapeutics. Science 297, 353–356.
Hauptmann, S., Keil, U., Scherping, I., Bonert, A., Eckert, A., Muller, W.E., 2006. Mitochondrial dysfunction in sporadic and genetic Alzheimer's disease. Exp. Gerontol. 41, 668–673.
Hoozemans, J.J., Veerhuis, R., Van Haastert, E.S., Rozemuller, J.M., Baas, F., Eikelenboom, P., et al., 2005. The unfolded protein response is activated in Alzheimer's disease. Acta Neuropathol. 110, 165–172.
Ishige, K., Takagi, N., Imai, T., Rausch, W.D., Kosuge, Y., Kihara, T., et al., 2007. Role of caspase-12 in amyloid beta-peptide-induced toxicity in organotypic hippocampal slices cultured for long periods. J. Pharmacol. Sci. 104, 46–55.
Kim, I., Xu, W., Reed, J.C., 2008. Cell death and endoplasmic reticulum stress: disease relevance and therapeutic opportunities. Nat. Rev. Drug Discov. 7, 1013–1030.
Kubo, T., Nishimura, S., Kumagae, Y., Kaneko, I., 2002. In vivo conversion of racemized beta-amyloid ([D-Ser 26]A beta 1-40) to truncated and toxic fragments ([D-Ser 26]A beta 25-35/40) and fragment presence in the brains of Alzheimer's patients. J. Neurosci. Res. 70, 474–483.
Li, P., Nijhawan, D., Budihardjo, I., Srinivasula, S.M., Ahmad, M., Alnemri, E.S., et al., 1997. Cytochrome c and dATP-dependent formation of Apaf-1/caspase-9 complex initiates an apoptotic protease cascade. Cell 91, 479–489.
Manczak, M., Mao, P., Calkins, M.J., Cornea, A., Reddy, A.P., Murphy, M.P., et al., 2010. Mitochondria-targeted antioxidants protect against amyloid-beta toxicity in Alzheimer's disease neurons. J. Alzheimers Dis. 20, s609–s631.
McCullough, K.D., Martindale, J.L., Klotz, L.O., Aw, T.Y., Holbrook, N.J., 2001. Gadd153 sensitizes cells to endoplasmic reticulum stress by down-regulating Bcl2 and perturbing the cellular redox state. Mol. Cell. Biol. 21, 1249–1259.
Millucci, L., Ghezzi, L., Bernardini, G., Santucci, A., 2010. Conformations and biological activities of amyloid beta peptide 25-35. Curr. Protein Pept. Sci. 11, 54–67.
Morishima, N., Nakanishi, K., Takenouchi, H., Shibata, T., Yasuhiko, Y., 2002. An endoplasmic reticulum stress-specific caspase cascade in apoptosis: cytochrome c-independent activation of caspase-9 by caspase-12. J. Biol. Chem. 277, 34287–34294.
Morsy, M.A., El-Moselhy, M.A., 2013. Mechanisms of the protective effects of curcumin against indomethacin-induced gastric ulcer in rats. Pharmacology 91, 267–274.
Nakagawa, T., Zhu, H., Morishima, N., Li, E., Xu, J., Yankner, B.A., et al., 2000. Caspase-12 mediates endoplasmic-reticulum-specific apoptosis and cytotoxicity by amyloid-beta. Nature 403, 98–103.
Paradis, E., Douillard, H., Koutroumanis, M., Goodyer, C., Le Blanc, A., 1996. Amyloid beta peptide of Alzheimer's disease downregulates Bcl-2 and upregulates bax expression in human neurons. J. Neurosci. 16, 7533–7539.
Paschen, W., Mengesdorf, T., 2005. Endoplasmic reticulum stress response and neurodegeneration. Cell Calcium 38, 409–415.
Ramalingam, M., Kim, S.J., 2012. Reactive oxygen/nitrogen species and their functional correlations in neurodegenerative diseases. J. Neural Transm. 119, 891–910.
Rath, K.S., McCann, G.A., Cohn, D.E., Rivera, B.K., Kuppusamy, P., Selvendiran, K., 2013. Safe and targeted anticancer therapy for ovarian cancer using a novel class of curcumin analogs. J. Ovarian Res. 11, 35–47.
Ron, D., Walter, P., 2007. Signal integration in the endoplasmic reticulum unfolded protein response. Nat. Rev. Mol. Cell Biol. 8, 519–529.
Sandur, S.K., Pandey, M.K., Sung, B., Ahn, K.S., Murakami, A., Sethi, G., et al., 2007. Curcumin, demethoxycurcumin, bisdemethoxycurcumin, tetrahydrocurcumin and turmerones differentially regulate anti-inflammatory and anti-proliferative responses through a ROS-independent mechanism. Carcinogenesis 28, 1765–1773.
Schroder, M., Kaufman, R.J., 2005. The mammalian unfolded protein response. Annu. Rev. Biochem. 74, 739–789.
Selkoe, D.J., 2001. Alzheimer's disease: genes, proteins, and therapy. Physiol. Rev. 81, 741–766.
Shearman, M.S., Ragan, C.I., Iversen, L.L., 1994. Inhibition of PC12 cell redox activity is a specific, early indicator of the mechanism of beta-amyloid-mediated cell death. Proc. Natl. Acad. Sci. U.S.A. 91, 1470–1474.
Sisodia, S.S., Annaert, W., Kim, S.H., De Strooper, B., 2001. Gamma-secretase: never more enigmatic. Trends Neurosci. 11, 2–6.
Slee, E.A., Harte, M.T., Kluck, R.M., Wolf, B.B., Casiano, C.A., Newmeyer, D.D., et al., 1999. Ordering the cytochrome c-initiated caspase cascade: hierarchical activation of caspases-2, -3, -6, -7, -8, and -10 in a caspase-9-dependent manner. J. Cell Biol. 144, 281–292.
Takuma, K., Yan, S.S., Stern, D.M., Yamada, K., 2005. Mitochondrial dysfunction, endoplasmic reticulum stress, and apoptosis in Alzheimer's disease. J. Pharmacol. Sci. 97, 312–316.
Tocharus, J., Jamsuwan, S., Tocharus, C., Changtam, C., Suksamrarn, A., 2012. Curcuminoid analogs inhibit nitric oxide production from LPS-activated microglial cells. J. Nat. Med. 66, 400–405.
Vembar, S.S., Brodsky, J.L., 2008. One step at a time: endoplasmic reticulum-associated degradation. Nat. Rev. Mol. Cell Biol. 9, 944–957.
Venkateswarlu, S., Ramachandra, M.S., Subbaraju, G.V., 2005. Synthesis and biological evaluation of polyhydroxycurcuminoids. Bioorg. Med. Chem. 13, 6374–6380.
Zawia, N.H., Lahiri, D.K., Cardozo-Pelaez, F., 2009. Epigenetics, oxidative stress, and Alzheimer disease. Free Radic. Biol. Med. 46, 1241–1249.
Zhang, D., Armstrong, J.S., 2007. Bax and the mitochondrial permeability transition cooperate in the release of cytochrome c during endoplasmic reticulum-stress-induced apoptosis. Cell Death Differ. 14, 703–715.